JOURNAL OF CATALYSIS 154, 222–229 (1995)

Reducibility of Rhenium in Pt–Re/Al_2O_3 Reforming Catalysts: A Temperature Programmed Reduction–X-Ray Absorption Near-Edge Structure Study

C. G. Michel,* W. E. Bambrick,* R. H. Ebel,* G. Larsen,†,[1] and G. L. Haller†,[2]

*CYTEC Industries, Research & Development, 1937 West Main Street, P.O. Box 60, Stamford, Connecticut 06904-0060; and †Department of Chemical Engineering, Yale University, New Haven, Connecticut 06520-8286

Received July 12, 1994; revised February 20, 1995

Temperature programmed reduction (TPR) experiments were performed on Pt–Re/Al_2O_3 catalysts in an X-ray absorption near-edge structure (XANES) apparatus to assess the effect of different metal loadings and different Re/Pt ratios on the reducibility of Re. It was found that these two variables affect the reduction kinetics of Re, but they do not seem to affect the final oxidation state of the Re metal. The performance of these catalysts under reforming conditions appears to correlate with the mode of metal particle generation of the samples, as monitored by the TPR–XANES technique. Catalyst performance data have been generated in a laboratory bench scale unit as well as in a pilot plant unit. The relative binding energy (BE) of core *p* electrons of Re in the catalysts with respect to an appropriate internal reference was monitored at both the L_{II} and L_{III} edges as a function of the reduction temperature. Such a comparison served as a test to confirm that the kinetics of Re reduction as monitored by the TPR–XANES technique is independent of the edge chosen. We were unable to obtain a precise two-shell fitting of the Pt–Re by EXAFS. This type of fitting is complicated by backscattering by oxygen in the alumina lattice after reduction, providing too large a number of independent parameters for a reliable fitting. © 1995 Academic Press, Inc.

1. INTRODUCTION

Bimetallic Pt–Re/Al_2O_3 catalysts for naphtha upgrading or reforming are widely used in the petroleum refining industry and have received considerable attention over the past two decades. Thorough reviews on the subject are presented elsewhere (1, 2). Recently, we have studied the reducibility of Pt and Re in bimetallic Pt–Re/Al_2O_3 catalysts by means of temperature programmed reduction (TPR) experiments in an X-ray absorption near-edge structure (XANES) (3). Our method consists of monitoring the relative binding energy (BE) of core electrons, arbitrarily taken as the first inflection point in the X-ray absorption spectrum, while applying a linear temperature ramp under H_2 flow. One advantage of following XANES BEs during TPR over the conventional H_2 consumption measurement by thermal conductivity detectors is that it permits us to follow the reduction kinetics of each metal independently. Coreduction of the two metals gives a convoluted H_2 consumption signal which does not provide direct information about the reduction chemistry of each component. In addition XANES, unlike EXAFS, is not affected by Debye–Waller factors. Therefore, it can be studied at different temperatures without affecting the signal/noise ratio.

Some of the findings of our previous study can be summarized as follows. At least for Re, we have shown that this method is less subject to artifacts than "white line" area analyses (3) and is probably less affected by final state effects than X-ray photoelectron spectroscopy (XPS). As in any other photon-in electron-out spectroscopy, XPS is expected to yield BE estimates that are strongly dependent on particle size, due to screening effects caused by the conduction band (4). We also noted that Pt-catalyzed reduction of Re in samples with a 1 : 1 Pt/Re ratio takes place around 300°C.

In this paper, TPR–XANES and EXAFS have been used to expand our previous study. The validity of our technique, with regard to the possibility of artifacts accompanying the experimental approach, was assessed by analysis of different absorption edges of Re. Factors affecting Re reduction and the structure of the metal clusters were monitored by this characterization tool on a series of bimetallic catalysts with different Re loadings and different Re/Pt atomic ratios.

With proper applications of surface pretreatment procedures, catalyst performance data have been generated in a laboratory bench scale unit as well as in a pilot plant unit. In both units, operating at low S levels, the expected

---

[1] Current address: Department of Chemical Engineering, University of Nebraska, Lincoln, NE 68510.

[2] To whom correspondence should be addressed.

0021-9517/95 $12.00

performance benefit of high-Re catalysts (with a Re/Pt ratio greater than one) was achieved. For the series of high-Re catalysts tested in this study, some features of the metal cluster microstructures are discussed for the optimum Re/Pt atomic ratio. In the discussion that follows, we will use terminology that applies to commercial catalysts which are said to have a low loading, e.g., 0.3 wt% Pt, and a balanced Re/Pt ratio, i.e., Re/Pt = 1. Metal ratios with Re/Pt > 1 are called skewed and, in order to make EXAFS possible, some of our samples had high metal loading (1–2 wt%) relative to commercial catalysts.

In this work, we have concentrated on Re L_{III} XANES, which provides better signal to noise ratios than Pt L_{II} (see Ref. (3) for a discussion of TPR–XANES on both metals). While it is desirable to perform EXAFS as well as XANES on the same sample, EXAFS is not feasible when commercial loading is used, but we do provide some EXAFS analysis on catalysts with loadings several times that used commercially (but with the same Re/Pt ratios used commercially).

2. EXPERIMENTAL

2.1 Catalyst Preparation

All the catalyst samples used in this study, except those used in the pilot plant work, were prepared by impregnation of extruded γ-alumina substrate using an aqueous solution of chloroplatinic acid (H_2PtCl_6), perrhenic acid($HReO_4$), HCl, and HNO_3. The substrate, supplied by Criterion Catalyst Company, was of >99.9% purity with a typical surface area of 200–220 m^2/g and a pore volume of 0.6 cm^3/g. The impregnation was performed in a lab scale rotary evaporator with an amount of solution in excess of that needed to fill substrate pores, and the impregnated alumina was dried at 80°C for a few hours (3). The catalyst was further activated by staged drying and a final calcination of 525°C for about 1 h.

2.2 X-Ray Absorption Measurements

The X-ray absorption spectroscopy experiments at the L_{II}–L_{III} edges were performed at the C-II station of the Cornell High Energy Synchrotron Radiation Source (CHESS, 5.3 GeV, 70–30 mA ring current). The Si 220 monochromator slits were set to give a spectral resolution around 1–1.2 eV energy range for XANES measurements and around 4 eV for EXAFS scans. A 20% detuning of the monochromator signal off the maximum was carried out in order to decrease the relative intensity of higher harmonics of the beam. Conventional ion chambers filled with either N_2, Ar, or N_2/Ar blends were used as detectors. The choice of gas composition in each chamber was governed by signal/noise requirements. In order to account for the typically poor reproducibility of the mechanical setting of the crystal angle, a XANES internal standard arrangement was set up in the following sequence: ion chamber 1 (monitor)–sample (cell)–ion chamber 2 (detector 1)–reference material (Pt foil or Re powder)–ion chamber 3 (detector 2). In this way, it was possible to determine BEs relative to the internal reference by simply comparing log (mon/det_1) versus log(det_1/det_2) (sample and reference absorption, respectively) at the absorption edge, arbitrarily taken as the inflection point. Additional details on X-ray absorption measurement of the Pt and Re BE may be found in Ref. (3). We have found that it is of crucial importance to limit the solid angle subtended by the reference material with respect to the second ion chamber because contamination of the sample log(mon/det_1) signal at the edge of fluorescence radiation from the reference would otherwise be present. The latter phenomenon is typically observed in the form of a pre-edge "dip" (2–6 eV before the absorption edge inflection point) of variable intensity, but can easily be prevented by simply increasing the separation between det_1 and det_2, or by allowing a slit the size of the beam to exit det_1.

Self-supported catalyst disks with appropriate optical thickness (μd_{total} = 1.9) were placed in the X-ray absorption spectroscopy (XAS) cell and dried under an air flow for 1/2 h at 180°C prior to a TPR run or a reduction cycle before EXAFS data collection. In the case of XANES data acquisition, the temperature in the cell was stabilized at the desired initial value for a TPR run and a 5% H_2 in N_2 mixture (reducing gas) was then introduced. The cell was purged for 10 min under that gas stream before a 5°C/min temperature ramp was applied and scans were taken every 2 min around the selected Re edge. The temperature was ramped in this fashion up to 650°C, where Re reduction was completed. The BE can be determined with a computational error of 0.2 eV. For EXAFS, the catalyst disk was pre-reduced for 1 h at 550°C under flowing 5% H_2/He.

An example of raw data for one sample, 0.3 wt% Pt–0.3 wt% Re/Al_2O_3 (labeled bPtRe, see Table 1), is shown in Fig. 1. The acquisition time for XANES scans was 2 min, equivalent to a 10 K temperature resolution in our XANES–TPR experiments. In Fig. 2, we show an example of $\chi(k)$ which is k^2 weighted and normalized, but the obvious experimental glitch has not been removed to indicate the quality of the data. Because EXAFS required loadings higher than commercial catalysts, this example is for 0.9 wt% Pt–1.8 wt% Re/Al_2O_3 catalyst (labeled hlsPtRe, see Table 1). These data are the result of averaging three scans of approximately 25 min acquisition time.

2.3 Catalyst Selection and Pretreatment

A series of bimetallic catalysts with different Re to Pt atomic ratios were selected for study. The chemical

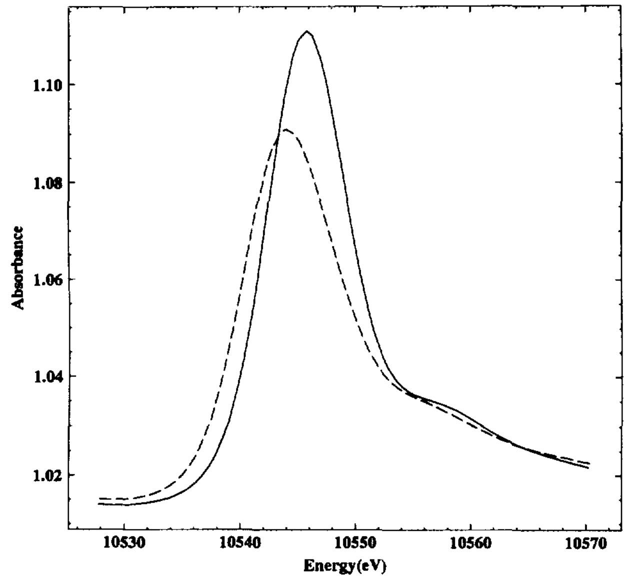

FIG. 1. Raw data for the Re L_{III} absorption edge of 0.3 wt% Pt–0.3 wt% Re/Al_2O_3. The solid line is before reduction and the dashed line is after reduction. The inflection points of the edges have been positioned with respect to an internal standard of Re metal scanned simultaneously.

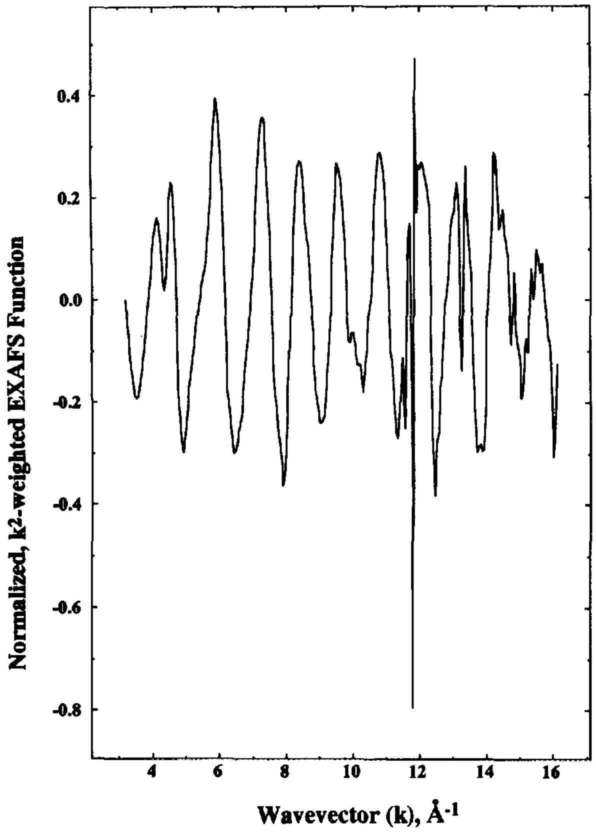

FIG. 2. The $\chi(k)$ EXAFS function of Re L_{III} 0.9 wt% Pt–1.8 wt% Re/Al_2O_3 after normalization and k^2 weighting. The glitch at about k = 11.8 Å^{-1} would be removed before analysis.

TABLE 1

Catalyst Samples Prepared

Pt wt%	Atomic ratio Re/Pt	Metal loading	Type	Notation[a]
0.3	1	Low	Balanced	bPtRe
0.22	1.5 1.7 1.8 1.9 2.0	Low	Skewed	sPtRe
0.22	2.9	Low	Super skewed	ssPtRe
1.8	1	High	Balanced	hlbPtRe
0.9	2	High	Skewed	hlsPtRe

[a] Here b means balanced, s means skewed, ss means super-skewed, hlb means high-loading balanced, and hls means high-loading skewed.

compositions of Pt in wt% and Re/Pt atomic ratio for these catalysts are shown in Table 1.

Catalyst precursors in oxidic form were reduced in a dry environment that favored catalytic reduction of Re by Pt. Following reduction, the catalyst samples were sulfided with dilute H_2S at 525°C until a threefold to fivefold excess over that needed to form Re_2S had passed over the catalyst. The catalyst pretreatment procedure and the process conditions for reduction and sulfidation are described in detail in Ref. (2).

2.4 Catalyst Testing

Catalyst samples were tested in two different-sized units, a laboratory bench scale unit and a pilot plant unit. Most of the testing was done in the bench unit. The pilot unit was used only to verify the conclusions reached by use of the bench unit.

The bench unit was operated with pure H_2 on a once-through basis; i.e., no gas was recycled. Feedstock was a blend of reagent grade hydrocarbons containing less than 100 ppb of S. Tests were run 200 psig; other conditions are shown in Table 2. For both the bench and pilot units, gas chromatography was used to determine reactor effluent composition. A 50-m PONA gas chromatography capillary column, Part Number 9091A-001, supplied by Hewlett–Packard, was temperature-programmed to resolve C1–C10 hydrocarbons detected using a flame ionization detector. Gaseous reactor effluent was injected via a 1-ml sample loop and transferred through heated lines to the Hewlett–Packard 5890 gas chromatograph for analysis. From the composition, the octane number was computed for each test condition (5). For the bench unit, activity was defined as the temperature needed to achieve 99 octane on fresh catalyst. Catalyst activity decline rate was the

TABLE 2

Test Conditions—Bench Scale Unit

LHSV	2
H_2/HC ratio	5
Feedstock	Blend of *n*-heptane, methylclopentane, methylcyclohexane, and toluene, containing 63 vol% paraffin, 24 vol% naphthenes, and 13 vol% aromatics
Activity mode	
Temperature ramp	Stepwise 500–530°C
Octane range	~95–102
Duration	28 h
Stability mode	
Temperature	Isothermal, selected to give 99 octane at start of run
Duration	About 100 h
Reformate analyses	Gas chromatograph every 3 h

isothermal octane decline rate as measured every 3 h chromatographically from 99 octane at the start of the run. Catalyst lifetime was arbitrarily defined as the negative reciprocal of the octane decline rate.

The pilot plant test unit was operated with a recycle H_2 stream. Feedstock was a full boiling range naphtha. Rhenium-containing reforming catalysts are sensitive to poisoning by S. The sensitivity increases as the Re/Pt ratio increases (6). The two sources of sulfur, S in the feedstock and H_2S from presulfiding, can build up excessive levels of H_2S in the recycle stream. Therefore the feedstock was pretreated by drying it over molecular sieves and then passing the naphtha through two columns packed with small nickel particles, one hot and one at room temperature. This reduced the S in the naphtha from about 2 ppm to less than 100 ppb. As a further precaution, the gas recycle stream in the test unit was passed through a ZnO/Al_2O_3 sulfur trap. The pilot unit was operated at 150 psig, LHSV of about 2, and H_2/HC ratio of about 4; see Table 6. A charge of 50 ml of prereduced and sulfided catalyst was diluted with inert solids and charged to the stainless steel reactor. The temperature profile was maintained relatively isothermal during testing. At the start of the run, temperature was adjusted to give a reformate octane of 100. Catalyst aging rate is defined as the temperature increase per hour required to maintain the reformate at 100 octane.

3. RESULTS & DISCUSSION

3.1 EXAFS Analysis

In trying to derive independent structural parameters for Pt and Re in Pt–Re catalysts from EXAFS data, we encountered the same difficulties as previosuly described by Sinfelt *et al.* (7, 8), namely, a strong correlation between the coordination numbers and the Debye–Waller factors. This is mainly due to the fact that Pt and Re, two elements with very similar atomic numbers, are very much alike in terms of physical properties such as EXAFS backscattering amplitude and phase shift functions. The resulting fittings that would otherwise give the EXAFS parameters typically showed many local minima of comparable quality (no unique solution). This situation prevented us from obtaining independent absolute coordination numbers (N), but the two-metal first-shell modeling of the Re $L_{\rm III}$ EXAFS on both hls (high-loading skewed, see Table 1) and hlb (high-loading balanced, see Table 1) Pt–Re catalysts generally gave a $N_{\rm ReRe}/N_{\rm RePt}$ ratio in the range 2–3. This is in agreement with previous data (7), and is consistent with the idea that the Pt–Re particles are segregated or that a small amount of pure Re phase is present in the final catalyst. The choice of the edge used for EXAFS analysis was not arbitrary. The Re $L_{\rm III}$ edge is the only L-type transition among the six possible in the Pt–Re system that does not overlap with the other absorption lines by as much as 1000 eV. The use of the first 400–500 eV of the Pt $L_{\rm III}$ edge has been previously suggested for modeling the Pt/EXAFS in $Pt–Re/Al_2O_3$ catalysts (9), but it is important to point out the resolution limitations of such a small spectral range and the overall validity of the conclusions derived from its analysis.

To further illustrate the physical limitation outlined above regarding the physical similarity of Pt and Re, we have modeled the metal–metal contribution to the first shell around Re as a single metal (M) scatterer using reference functions extracted from both Re powder and Pt foil (see Table 3). Very recently, Caballero *et al.* (10) have used this approach to carry out *in situ* EXAFS measurements aimed toward modeling the effect of coking (formation of M–C bonds) under reforming conditions. The best fits to the EXAFS data of hlb and hls catalysts presented in Table 3 show that, apart from the Re–M average coordination distance, there is little effect on either N or the Debye–Waller factors. The modeling of data was carried out by a similar technique pioneered by Koningsberger *et al.* (11). In brief, a higher order k-

TABLE 3

EXAFS Modeling of Re $L_{\rm III}$ Data on hlsPtRe and hlbPtRe Catalysts

Sample	$N_{\rm M\text{-}M}$	DW_f (Å^2)	$R_{\rm M\text{-}M}$ (Å)
hlsPtRe[a]	4.8	0.0026	2.75
hlbPtRe[a]	5.4	0.0028	2.76
hlsPtRe[b]	5.1	0.0027	2.72
hlbPtRe[b]	5.1	0.0026	2.72

[a] Using Re powder as reference.

[b] Using Pt foil as reference.

TABLE 4

Re–O EXAFS Modeling

Sample	$N_{Re\text{-}O}$	DW_f (Å^2)	$R_{Re\text{-}O}$ (Å)
hlsPtRe	2.0	0.0028	2.20
hlbPtRe	1.5	0.0014	2.24

weighting of data guarantees that the contribution of third-row transition elements such as Pt and Re becomes completely dominant in the range of say, 8–16 Å^{-1}. The remaining low-k parts of the spectra are then fit for oxygen or any other lower atomic number backscatters that may contribute to the overall EXAFS signal. In the case of Re L_{III} EXAFS, we found that oxygen backscattering cannot be discarded, and we proceeded to model the low-k region (Table 4). The modest Re–O coordination observed in both catalysts suggests that the less nobel metal plays a part in the anchoring of the metal particle to the support, but clearly does not contribute to the formation of an ordered raft or rug structure. Such an arrangement of metal atoms on the alumina surface would require an oxygen coordination of about 3.

3.2 TPR-XANES Analysis

Figure 3, a–c shows a plot of the Re L_{III} edge relative BEs (ΔBE) versus reduction temperature for the three low-loading catalysts. It can be seen that a BE shift of about 0.2 eV relative to Re bulk is achieved after reduction above 550°C, independent of the Re/Pt ratio. We have found that ΔBEs in Re–O compounds are directly related to the oxidation state (3). The small 0.2 eV shift observed lies within the experimental error of the technique and allows us to conclude that Re reaches the metallic state after a complete reduction cycle. The very small changes at temperatures around 500°C are due to reduction of Re that has not been catalyzed by Pt (3). A more interesting picture that resembles the conventional rate of H_2 consumption TPR curves is obtained when the first deriva-

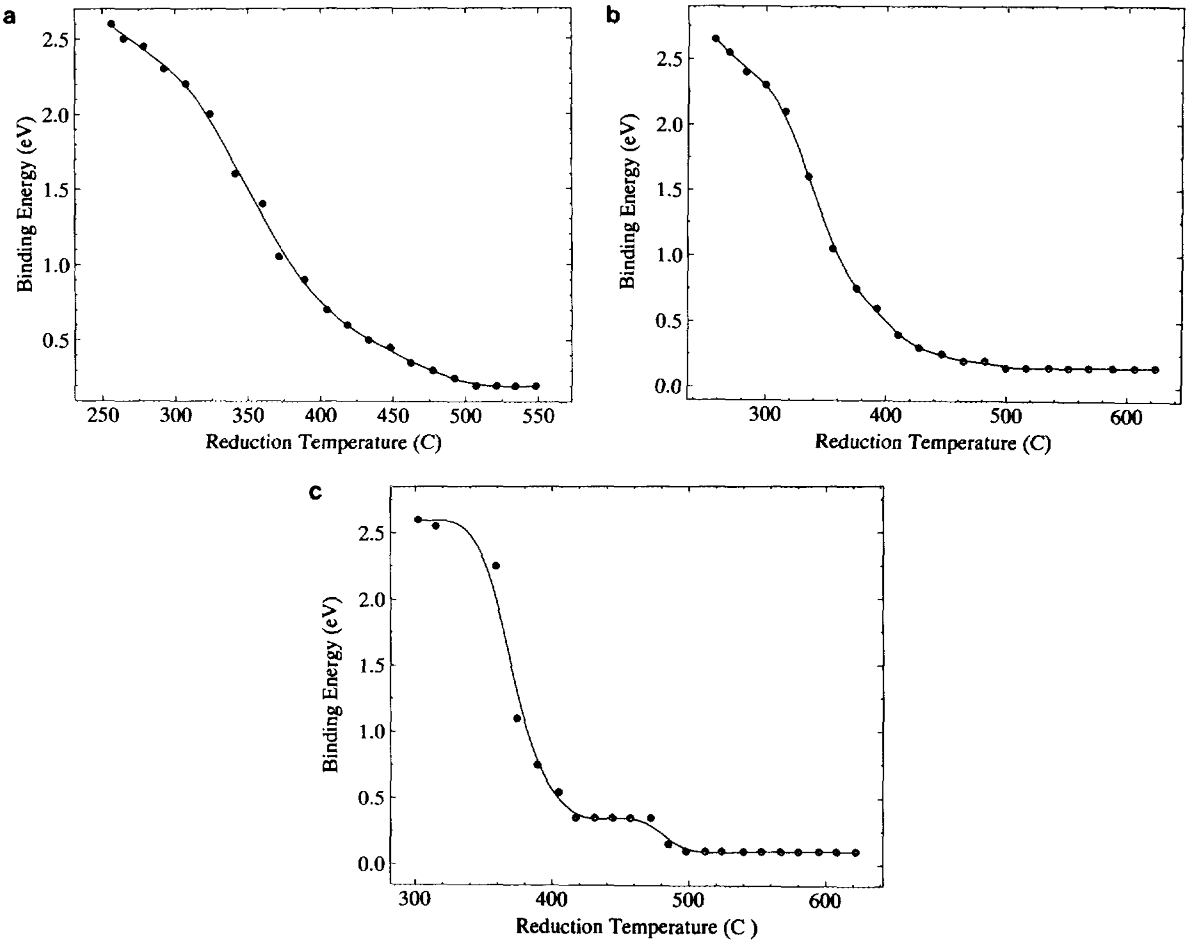

FIG. 3. (a) TPR-XANES of the Re L_{III} edge of 0.3 wt% Pt–0.3 wt% Re/Al_2O_3 catalysts. (b) TPR-XANES of the Re L_{III} edge of 0.22 wt% Pt–0.44% Re/Al_2O_3 catalysts. (c) TPR-XANES of the Re L_{III} edge of 0.22 wt% Pt–0.64 wt% Re/Al_2O_3 catalysts.

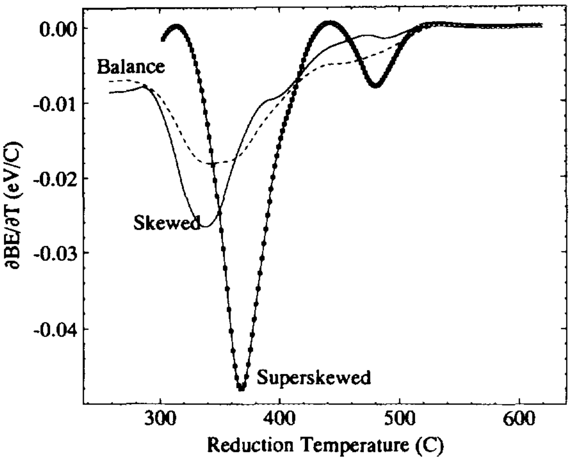

FIG. 4. The derivative curves from Fig. 3, a–c.

tives of the curves in Fig. 3, a–c are taken (Fig. 4). Such BE versus temperature plots give an idea of the rate of change in the Re oxidation state during the reduction process. At least two features are immediately apparent and they are both related to the unique reduction behavior of the catalyst with the highest Re/Pt ratio. First, the contribution of the noncatalyzed Re reduction to the TPR profile (high temperature peak) is more pronounced in the case of super-skewed catalysts (ssPtRe, Re/Pt = 2.9), suggesting that a larger fraction of monometallic Re particles are present in the latter. In addition, the Pt-catalyzed peak shifts toward higher temperatures with respect to both balanced and skewed catalysts (bPtRe and sPtRe, respectively; see Table 1).

Because H_2 spillover from Pt particles is not the dominant mechanism of Re reduction in this family of catalysts (2), the observed differences must be caused by other effects. We have recently found that even after the catalyst precursor is dried, essentially all Re is coreduced with Pt at around 300–340°C when the Cl content in the catalyst is kept to around 1 wt% (3). This also becomes evident in Fig. 4, at least for the sPtRe and bPtRe cases. This observation leads us to speculate that oxychloride species indeed play a role in the Re reduction process, as long as the Cl content is higher than those probably present in the catalyst in Ref. (10). The idea of a mobile Re-oxychloride precursor has been proposed previously by Shum *et al.* (12). Therefore, it is reasonable to think that a Cl deficit in the ssPtRe sample is responsible for the late reduction (decreased mobility) of Re, as well as the larger monometallic Re reduction peak. Another possible explanation would be that, since the ssPtRe catalyst contains the smallest amount of Pt of all the samples, it is a deficit in reduction sites rather than a Cl deficiency that causes the shift of the Pt-aided reduction peak toward higher temperatures. We tend to favor the second interpretation for reasons that will become appparent below. In any case, such a catalyst may well be expected to behave a priori differently under reforming conditions when compared to sPtRe and bPtRe. This was confirmed by carrying out catalytic tests on all three samples.

First, there is the problem that Re–S particles, resulting from presulfiding of a reforming catalyst with a pure Re phase, will have an enhanced activity for hydrocracking and hydrogenolysis (13). Second, extreme S sensitivity is expected for catalysts containing Re/Pt ratios of 2 or higher (see Fig. 5), to the point that S concentrations above 250 ppb in the naphtha feed would severely compromise the normal operation of a reformer using high Re catalysts (1). In summary, while we believe that the balanced and the skewed catalysts used in this study contain 1 : 1 and 1 : 2 bimetallic particles, respectively, and little or no pure Re phase (see Fig. 4), such Re particles may be present in the super-skewed sample. The difference in the coreduction temperature of the latter with respect to both bPtRe and sPtRe could also have some structural implications that may relate to the poor performance of superskewed catalysts.

Figure 6 shows the TPR–XANES derivative curves of the hlbPtRe and hlsPtRe catalysts. It is immediately noticed that the Pt-catalyzed Re reduction shifts to temperatures about 40°C lower than those seen with low-loading samples in Fig. 4. Note that in this case, we have kept both Re and Cl content constant, while setting the high-loading balanced and skewed Re/Pt ratios by only adjusting the Pt wt% in the samples. In any event, Pt-catalyzed reduction of Re in the balanced catalyst occurs at about 20°C lower than in the high-loading skewed sample. Taking into account that the relative amount of Cl (Cl/Re) is lower in the high loading catalysts, it is therefore

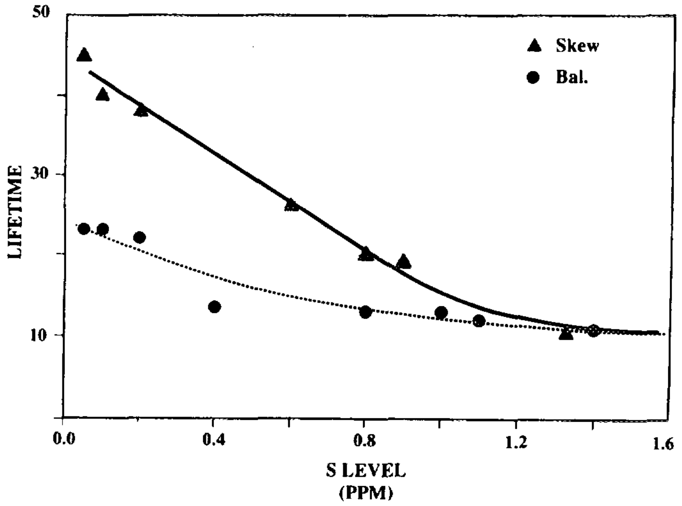

FIG. 5. Catalyst lifetime (negative reciprocal of the octane decline rate, hours per unit octane) as a function of the sulfur level in the feed for balanced and skewed catalysts.

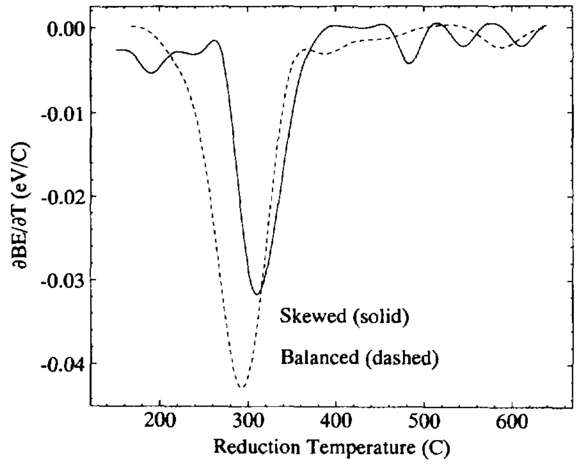

FIG. 6. Comparison of the derivatives of Re binding energy TPR curves for a balanced, high-loading catalyst (1.8 wt% Pt–1.8 wt% Re/Al_2O_3) compared to a skewed high-loading catalyst (0.9 wt% Pt–1.8 Wt% Re/AL_2O_3).

TABLE 5

Catalyst Life Testing (Bench Scale Unit)

Catalyst type	Atomic ratio Re/Pt	Relative lifetime[a]
Balanced	1	Reference = 1
Skewed	1.5	1.4
	1.7	1.8
	1.8	1.7
	1.9	2.1
	1.9	2.1
	2.0	2.0
	2.0	2.0
Super-skewed	2.9	1.5

[a] Catalyst lifetime is defined as the negative reciprocal of the octane decline, see text.

the concentration of reduced Pt sites on the surface rather than the Cl content that causes the small shifts observed, as long as the absolute amount of Cl is kept around 1 wt%. In other words, we are inclined to believe that oxychloride species with different Cl contents are not responsible for the observed temperature shifts in the reduction maxima, and more than one type of such species exists, they do not appear to be distinguishable from the redox chemistry viewpoint.

In another run, we also studied the TPR–XANES of Re in the hlsPtRe catalyst at both the L_{II} and the L_{III} edges. The derivative curves are shown in Fig. 7. It is seen that the major TPR peak due to coreduction is reproducible within 10°C, but the small peaks due to pure Re reduction in the temperature range 500–600°C are difficult to resolve either as a triplet or a doublet (see Fig. 4 and 6 also). Therefore, we conclude that, in a semiquantitative fashion, the choice of XANES edge is not of crucial importance to follow the reduction kinetics of a metal by means of this technique.

3.3 Catalyst Testing

Test results for the catalyst samples in the bench scale test unit are shown in Table 5. Activity was practically invariant as the Re/Pt ratio varied from 1 to 3. However, catalyst life increased linearly as the Re/Pt ratio increased from 1 to 2. This corresponds to the interval where Pt-catalyzed reduction of Re is observed. Beyond a Re/Pt ratio of about 2, catalyst life falls off. This is the compositional region where noncatalyzed reduction of Re is observed. Catalyst life is adversely impacted when there is noncatalyzed Re reduction.

The importance of controlling the S at low levels is

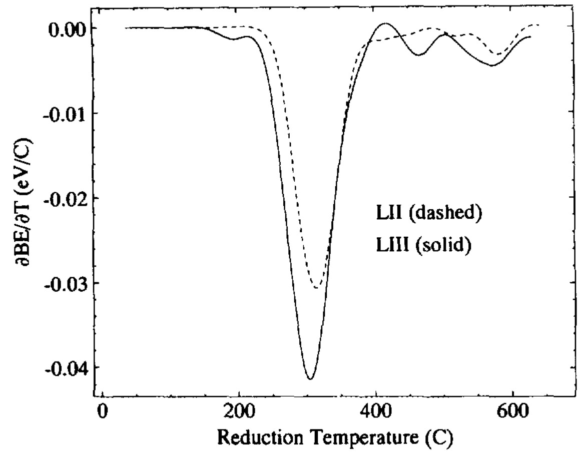

FIG. 7. A comparison of the derivatives of Re binding energy TPR curves observed at the L_{II} and L_{III} edges for a high-loading skewed (0.9 wt% Pt–1.8 wt% Re/Al_2O_3) catalyst.

TABLE 6

Test Conditions—Pilot Plant Test Unit

LHSV	~2
H_2/HC ratio	~4
Feedstock	Full boiling range naphtha with N + 2A characterization factor[a] ~50
Operating conditions	
Constant octane	Temperature adjusted to maintain 100 octane
Duration	Ten periods of 12 h each; total test time 120 h at 100 octane
Reformate analyses	Gas chromatography every 12 h

[a] Volume of naphtha plus two times the volume of aromatics divided by total volume.

shown in Fig. 5. These data points were obtained in the bench scale test unit. Note that at 1.0 ppm S the skewed catalyst shows little or no advantage over the balanced catalyst. At 0.2 ppm the skewed catalyst has about twice the life of the balanced catalyst.

The life of a catalyst with about 2/1 Re/Pt atomic ratio is about twice, by bench test, or 1.6 times, by pilot plant test, the life of a catalyst with 1/1 Re/Pt atomic ratio. Sulfur in the reforming system must be less than about 20 ppb for the longer life to be observed. From the evidence of XANES, TPR, and life testing, the sharp decline in catalyst life as the Re/Pt atomic ratio exceeds about 2 appears to be due to isolated, unalloyed Re particles.

4. CONCLUSION

The reduction behavior of Re is predictive of catalyst performance in bimetallic Pt–Re catalyst systems. As the Re/Pt ratio increases, catalyst lifetime increases only so long as catalyzed Re reduction takes place as measured by TPR–XANES. Appearance of a second Re phase, marked by high reduction temperature in the standard TPR and confirmed by the TPR–XANES, occurs as the Re/Pt ratio is increased above about 2. A decline in catalyst lifetime coincides with the appearance of the separate Re phase. Rhenium is only beneficial to the catalyst system when it is catalytically reduced by platinum. If S in the feed is controlled, a skewed (Re/Pt ratio of about 2) catalyst has about twice the lifetime of a balanced catalyst (Re/Pt ratio of about 1).

ACKNOWLEDGMENTS

The authors express their appreciation to Cornell High Energy Synchrotron Source for beam time which made this research possible. We also thank Dean Edgar (Criterion) for helpful comments, Robert Northcraft for supplying the alumina supports, and Tim Graver for pilot plant testing of our catalysts at the Criterion Manufacturing Facilities. Partial support at Yale University was provided by the DOE, Office of Basic Energy Sciences.

REFERENCES

1. Parera, J. M., and Figoli, N. S., *Catalysis* London **9,** 64 (1992).
2. Michel, C. G., Bambrick, W. E., and Ebel, R. H., *Fuel Process. Technol.* **35,** 159 (1993).
3. Hilbrig, F., Michel, C., and Haller, G. L., *J. Phys. Chem.* **96,** 9893 (1992).
4. Huizinga, T., and Prins, R. *Stud. Surf. Sci. Catal.*, **11,** 11 (1982).
5. Scherzer, J., *Catal. Rev. Sci. Eng.* **31,** 215 (1989).
6. Oyekan, S. O., McClung, R. G., and Moorehead, E. L., at AIChE Spring National Meeting, Houston, TX, April, 1991.
7. Via, G. H., Drake, K. F., Meitzner, G., Lytle, F. W., and Sinfelt, J. H., *Catal. Lett.* **5,** 25 (1990).
8. Meitzner, G., Via, G. H., Lytle, F. W., and Sinfelt, J. H., *J. Chem. Phys.* **87,** 6354 (1987).
9. Dexpert, H., Lagarde, P., and Bournonville, J. P., *J. Mol. Catal.* **25,** 347 (1984).
10. Caballero, A., Villain, F., Dexpert, H., LePeltier, F., and Lynch, J., *J. Chem. Soc. Faraday Trans.* **89,** 159 (1993).
11. Moller, K., Koningsberger, D. C., and Bein, T., *J. Phys. Chem.* **93,** 6116 (1989).
12. Shum, V. K., Butt, J. B., and Sachtler, W. M. H., *J. Catal.* **99,** 126 (1986).
13. Parera, J. M., Beltramini, J. N., Querini, C. A., Martinelli, E. E., Chiren, E. J., Aloe, P. E., and Figoli, N. S., *J. Catal.* **99,** 19 (1986).